Analysis of the Goose Point area near Lacombe, Louisiana, Validates New Geophysical Data Type—Natural Sourced Electromagnetism (NSEM)—for Detection of Lineaments Associated with Faults and Sedimentary Features

Kathleen S. Haggar, Les R. Denham, and Louis J. Berent

Dynamic Measurement, LLC, 211 Baker Rd., Ste. 382, Barker, Texas 77431

ABSTRACT

This newly patented natural sourced electromagnetism (NSEM) associated with lightning strike databases was used to reexamine an area previously interpreted by only conventional geological datasets. The available existing data was explored and integrated into a 3D framework of resistivity and permittivity data on a Landmark DecisionSpace™ workstation. This lightning data integration project resulted in the re-interpretation of mapped faults and the introduction of several new possible faults by correlating indicative patterns of resistivity and permittivity through the data cube. The Goose Point lightning data study area covers a 110 sq. mi (285 sq. km) near Lacombe, Louisiana. The surface of the study area encompasses the Pleistocene Prairie Allow Group, Holocene marsh, and a northeast segment of Lake Pontchartrain.

Based on the years of lightning data available from projects in Texas, Louisiana, North Dakota, Michigan, and Florida, we have learned that lightning strikes are not uniformly distributed and tend to cluster. Lightning strike locations and their associated attributes are primarily controlled by shallow geological modifications of the earth's terralevis (shallow) currents. These electrical currents are influenced by lateral geological inhomogeneity caused by faults, fractures, lithology, mineralization, gas, pore-fluids, and salinity variations. Though still in its infancy, lightning data is progressing towards becoming an effective reconnaissance tool in petroleum and mineral exploration as well as geo-hazard and environmental studies.

This study area was chosen because it exhibits all of the same land change and marsh break-up characteristics as observed across much of coastal Louisiana. However, Goose Point does not possess any of the same anthropogenic influences typically assigned as causing land loss/land change. Active faults associated with the Baton Rouge fault system, crustal down-warp, and sea level rise constitute the probable natural drivers for subsidence and land change in this area.

Existing datasets utilized in this study include: light detection and ranging (LIDAR), a geologic map of the region, high resolution sparker data, several shallow cores, three types of NSEM attribute data, and resistivity and permittivity data. Rise time, rate of rise time, and strike-density were used to identify and interpret lineaments and patterns related to known faults, transforms, and channel features.

The high resolution sparker data were used to tie surface fault interpretations to 3D lightning resistivity and permittivity volumes. Collectively, these ties and comparisons resulted in a re-interpretation of the existing fault data resulting in the identification of faults not previously mapped. While each region's geology is different, we now have more insight into the role and benefits of lightning strike data as a platform for linking sparse surface and shallow data types into an improved, more coherent interpretation of the subsurface.

Haggar, K. S., L. R. Denham, and L. J. Berent, 2015, Analysis of the Goose Point area near Lacombe, Louisiana, validates new geophysical data type— Natural sourced electromagnetism (NSEM)—for detection of lineaments associated with faults and sedimentary features: Gulf Coast Association of Geological Societies Transactions, v. 64, p. 139–153,

INTRODUCTION

A lightning database, now containing more than sixteen years of lightning strike data in the continental U.S., represents a new geophysical data type that can be used as a reconnaissance mapping tool for petroleum and mineral exploration, hydrology and geotechnical investigations, and geo-hazard identification. Lightning can be thought of as a form of naturally occurring electromagnetism (NSEM). A lightning strike is the breakdowns of the atmospheric dielectric between a charged cumulonimbus cloud and the earth. These surfaces form the two plates of a capacitor. As with seismic data, lightning can be analyzed in terms of specific attributes as this study will show. 3D Resistivity and Permittivity volumes are also generated and can be integrated with seismic and subsurface geology.

This paper documents a study area of approximately 110 sq. mi (285 sq. km) near Lacombe, Louisiana, called Goose Point. The surface in the study area includes Pleistocene Prairie Allow Group, Holocene Marsh, and Lake Pontchartrain. Here we compare selected lightning attributes—rise-time, rate-of-rise-time, and strike-density—with LIDAR high resolution elevation data. The various lightning attribute data reveal patterns and lineaments suggestive of channels, as well as meander features typically found on the Pleistocene Prairie surface. We also explore the application of lightning resistivity and permittivity volumes as tools to interpret and map possible faults in Lake Pontchartrain.

Main Menu
Search
Author Index
Papers
Help

DISCUSSION

Geologic Setting

The Baton Rouge–Denham Springs Fault System trends northwest-southeast, in echelon fashion, through the study area. This paper treats these faults collectively as the Baton Rouge Fault System. This sort of relay-of-motion of active surface faults parallels the observations of Dr. Carl Norman, Emeritus Geology Professor from the University of Houston, along the Long Point Fault and other faults to the northeast of Houston extending to the Woodlands area (C. Norman, 2015, personal communication). See Figure 1.

Active fault segments have been identified both onshore and in Lake Pontchartrain and many are mapped at the surface (Kindinger et al., 1999; Heinrich, 2004; Kulp et al., 2002; Kent and Dokka, 2013). Onshore segments have been mapped by the U.S. Geological Survey (USGS) and the Louisiana Geological Survey (LGS). The faults in the lake are largely mapped from geotechnical borings, cores, and/or high resolution sparker data by Jack Kindinger and others at the USGS (Kindinger; 1998; Lopez, 1997; Roth, 1999). Both the South Point Fault and the Goose Point Fault offset the Highway 11 Bridge and the Southern Railroad Bridge between Slidell and New Orleans. The South Point fault was known to be moving slowly, creeping for some time prior to repairs made to the railroad bridge in 1987. However, by 1996 both faults had offset the Railroad Bridge by about 2–3 in (5–7.5 cm). Subsidence rates vary between these faults over time with more overall movement occurring on the Goose Point Fault (Lopez, 1996).

Goose Point geomorphology is diverse and supports various habitats. Water features range in size from very small local drainage patterns to the main channel of Bayou Lacombe. Many abandoned stream channel meanders are etched in the landscape and can be imaged by finely scaled LIDAR. For decades, the marsh has been in transition to open water, much like the other coastal marshes across south Louisiana (Chabreck, 1956; Chabreck et al., 1978, 1988–90), and (Barras, various years, USGS Land Change maps). This progression reveals former river meanders and drainage patterns as the top marsh layers die off and are exported from the marsh.

Goose Point is unique in that it lacks the anthropogenic influences often cited as causing the loss of the coastal delta marshes. Subsidence models (Ivins and Dokka, 2007) indicate subsidence rates of the deep crust along the north shore of Lake Pontchartrain to be in the 3–4 mm/yr range with error bars of +/- 2 mm/yr. Other areas of the coast are significantly higher. Actual measurements between New Orleans East and Slidell average about 1.6 mm/yr (Ivins and Dokka, 2007). Recent presentations by Chris McLindon also highlight the relationship between the movement along the surface faults and fault trends and the dramatic land change across the Mississippi delta and its Holocene ancestors (McLindon, 2015, personal communication).

The shallow subsurface is still not well understood or well imaged. Well data is mostly limited above 2500 ft (762 m). Few companies recorded logs through the shallow data. At this stage of Goose Point investigation, we are just beginning to acquire digitized well log data, therefore well logs are not a part of the present study. In a project underway at Brigham Young University (BYU) by Jesse Dean Shumway, additional data will be incorporated into the Landmark Decision SpaceTM, such as well logs, maps of pay zones and paleo horizons, and faults. The Louisiana Department of Natural Resources (LA DNR) Well Log Library and SONRIS are the pri-

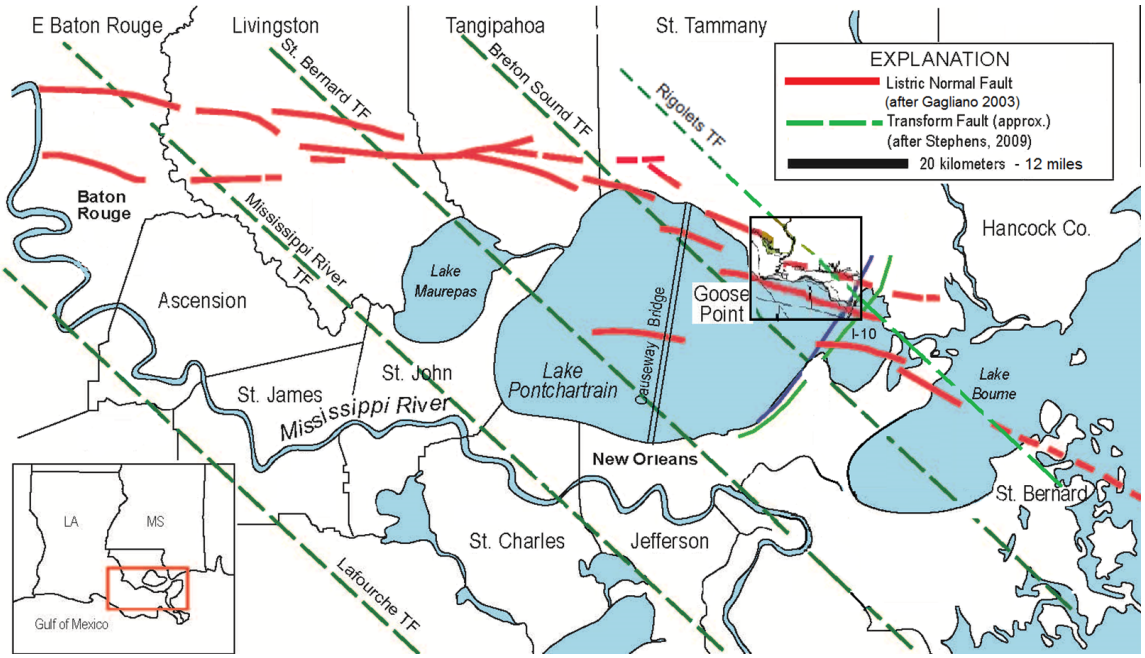

Figure 1. Index map showing 110 sq. mi (285 sq. km) study area as box over Goose Point. The inset black rectangular image locates a referenced LIDAR map for comparison to other maps. The red dashed lines show fault segments along the Baton Rouge Fault System after Gagliano et al. (2003) and the green dashed lines show the approximate locations of transforms after Stevens (2009).

mary sources for well logs, paleontology data, and base maps. NSEM resistivity and permittivity volumes will also be part of future studies.

Surfaces evaluated in the study area includes the Pleistocene Prairie Allow Group, Holocene Marsh, and Lake Pontchartrain (Heinrich et al., 2004). The surface units in the Goose Point area correspond to Holocene coastal marsh deposits (Hcm), relic Pleistocene coastal ridges (Ppec), undifferentiated Quaternary deposits (Qctu), and Prairie Allogroup of the Hammond alloformation (Pph). Excerpts from that map are shown in Figure 2 beside lightning attribute maps. The Prairie Allogroup is assigned to the Late Sangamon Stage in the LGS Fontainebleau Stratigraphic Chart (McCulloh, 2011).

Lightning Data

Lightning is a meteorological event and occurs over all geographic regions; land, marshes, and open water. Even though the height of the clouds, the intensity of the storms, and other meteorological effects change, the earth is a constant. Lightning is a form of naturally occurring (sourced) electromagnetism (NSEM). A lightning strike is the breakdown of the atmospheric dielectric between a charged cumulonimbus cloud and the earth, which together form two plates of a large capacitor (L. Denham, 2015, personal communication). However, precisely where lightning strikes the ground has been demonstrated to be primarily due to geologically controlled shallow earth currents. Geology, absent some catastrophic event, does not change and at the near surface conducts terralevis (shallow) earth currents (Nelson et al., 2013). These facts have spurred research resulting in the development of various techniques for data mining the lightning database for natural resources exploration (Dynamic Measurement, 2013) (Haggar et al., 2014).

The raw lightning data for this study was sourced from the National Lightning Detection Network (NLDN) which is owned by Vaisala, a Finnish company. The NLDN ground based lightning sensor network consists of about 110 detectors in the lower 48 states and is sufficient to record lightning strikes across virtually all of the U.S. Typically, strikes in Louisiana are recorded by 9–15 sensors in our study area.

Individual strike location data, rise time, peak current, peak to zero, are all measurements directly recorded by sensors in the NLDN. Once collected, additional proprietary algorithms are applied to the raw data and result

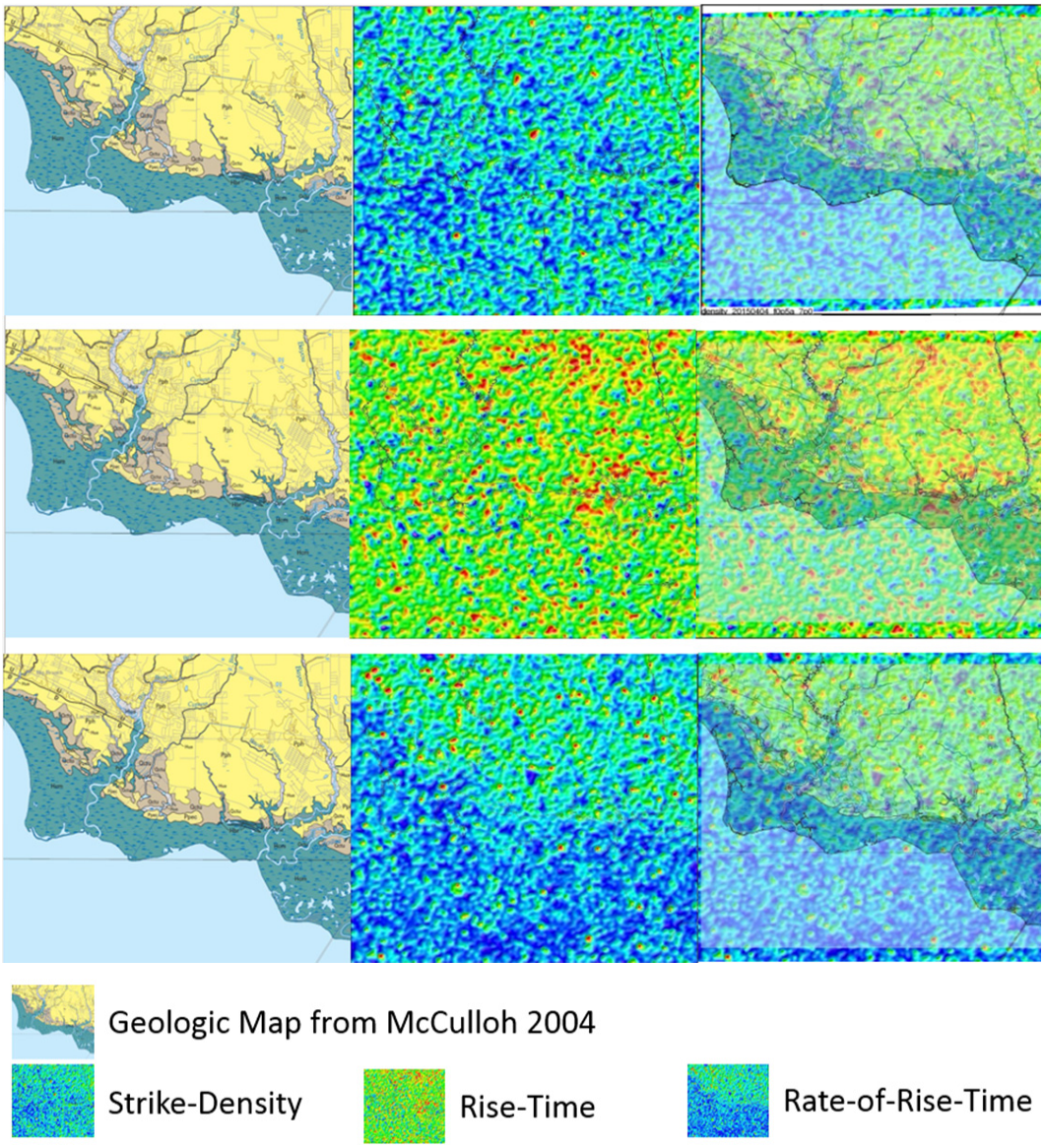

Figure 2. This panel shows the geologic map of the study area compared to strike-density (top row), rise-time (middle row), and rate-of-rise-time (bottom row).

in statistical values for each strike as well as the strike's relationship to the data set. Each lightning strike has a unique set of attributes which relate to the actual data recorded by the sensors.

Strike-density, rise-time, and rate-of-rise-time attributes, as well as two rock property volume attributes—Resistivity and Permittivity—are studied in this paper. The attributes are displayed as individual maps and reflect surface and possibly subsurface features. Lineaments seen in the basic attribute data are suggestive of channels and meander features, as well as relic beach trends on the Pleistocene Prairie surface. Resistivity and permittivity volumes provide a framework and subsurface link to sparker's previously mapped surface faults and bridge offsets data. Geohazards associated with gas in high resistivity amplitude areas require additional research. Additional field mapping will expand the Big Point Field *Siphonina davisi* sand structure map from Cullinan (1969).

Role of Sparker Data in this Goose Point Lightning Investigation

Sparker data has been the primary technology used to investigate shallow faults and channels in the lake due to its relatively low acquisition and processing costs. The USGS shot a loose grid of "sparker lines" in Lake Pontchartrain from 1994 to 1998. The primary purpose of investigating sparker data in this lightning study is verifying fault picks used to interpret fault in resistivity volumes. Resistivity and permittivity volumes will be discussed in a later section. Sparker data is only useful for interpretation of the shallowest geology. It does allow identification of some of the surface and near-surface expressions of faults reaching the lake bed.

While there are numerous 2D seismic lines in the lake, there is no known 3D seismic in the lake. Most seismic is not designed with any interest in imaging the shallow geology. In some data, this is an inherent acquisition problem which cannot be resolved by reprocessing the old lines. Where surface information might be extracted from seismic, it is generally cost prohibitive for academic research.

There are portions of nine sparker lines recorded 1994 to 1997 by the USGS incorporated into this study. These data were originally collected using an "electromechanical acoustic source," commonly called a "boomer" seismic source (Roth, 1999). "Noise" is expected with this type of seismic acquisition. Sparker data relies on an energy source that is relatively weak. Recorded data is restricted to a 60 to 100 ms (two-way time) record length, equivalent to depths of 147–246 ft (45 to 75 m), assuming a velocity of 4900 ft/s (1500 m/s). This original USGS sparker data quality is fair to poor. Over the years, much of the detailed information on data acquisition has been lost and is no longer available from the sparker contractor or the USGS (Kindinger, 2014, personal communication). While there are a considerable number of 2D seismic lines that run through the lake, to our knowledge, none have been released for publication. Dynamic Measurement, LLC (DML) used the USGS, publically available, digital SEG–Y data to reprocess lines 18a–b, 63a–b, and line 19. Reprocessing included phase rotation, a structural filter, and applying a root mean square (RMS) gain to improve horizontal continuity and data appearance. The reprocessed lines were loaded into Landmark's DecisionSpace™ along with the lightning data resistivity and permittivity volumes.

USGS core datasets have provided the ties to stratigraphic information such as the Top of the Pleistocene and the Pleistocene-Holocene Unconformity. Figure 3 shows the tie to the Pleistocene-Holocene surface on sparker line 19 with an overlay from Roth's (1999) interpreted data. The Top Pleistocene has been a difficult surface to map due to the discontinuous data across sparker lines and sparse core data. Based on a interpreted fault cuts on the available USGS sparker lines, the Goose Point fault off the tip of Goose Point has been interpreted as a continuous fault extending approximately 15 mi (24 km) to the east and also causing the offset of the Hwy. 11 Bridge (Lopez, 1997). The interpreted Goose Point fault imaged by sparker data offsetting the rail road trestle and the Highway 11 Bridge was also validated by Lopez (1997). Reprocessed sparker lines confirmed the faults although line 19 the fault was better imaged and picked slightly to the south of the original sparker pick used by Roth (1999).

Roth's (1999) illustration of the USGS "Poor Seismic/No Dredge Zones Map" is a useful interpretive tool for insights into both sparker and lightning interpretations. She concluded poor sparker data could be due to a variety of factors including acquisition errors, possibly sediment in the water column, gas charged bottom sediments, and relic disturbed zones created by dredging. By contrast, Rangia clam clusters and small patchy oyster reefs could result in zones that make bright reflectors with or without multiples.

Early studies of brines in the Baton Rouge aquifer associated with the Baton Rouge Fault movement were conducted by Rollo (1969), Kazmann (1970), and Kuecher et al. (2001). These studies concluded that some seismic sub-surface anomalies were directly related to the migration of gasses and brines migrating up fault planes of active faults. In some cases the anomalies continued to the surface.

Keucher et al. (2001) concluded that the Golden Meadow and the Lake Hatch fault zones were actively moving faults responsible for resistivity/EM (electromagnetic) anomalies. The Gas Research Institute contracted with the Argonne National Laboratory for an EM data collection that involved random resistivity soundings in their study area. By mapping the electrical data, and considering that clays are more conductive than sands, Argonne surmised that the upthrown side of the faults were more sand rich and the downthrown side were more clay rich. Saribudak (2011) reported similar observations of sands upthrown and shales downthrown across faults at the surface in his study of active radial faults from the Hockley salt dome near Katy, Texas. Like Keucher et al. (2001), he used a conventional resistivity profiles to generate his interpretations.

Stoessell and Prochaska (2005) reached their conclusions about the active nature of the Lacombe Segment of the Baton Rouge Fault in Lacombe, Louisiana, by studying the nature of brines along the fault plane in shallow aquifers. They concluded that the brines were not in situ based on their chemistry, which was actually more consistent with Miocene brines. These migrating fluids influence the area near the fault plane and could locally affect both seismic and EM responses near fault planes.

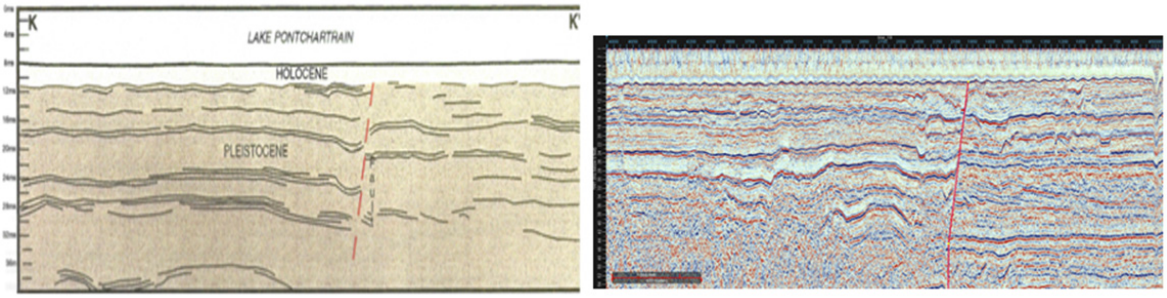

Figure 3. Comparison of interpreted sparker line 19 from Roth with DML-reprocessed sparker line.

Main Menu
Search
Author Index
Papers
Help

Tying Sparker to Lightning Resistivity and Permittivity

At Goose Point we have no EM similar to that of Kuecher et al. (2001) or Saribudak (2012), but we do have lightning data which is naturally sourced electromagnetism (NSEM). This is the first published Louisiana study to explore the adaptation of NSEM data to geological interpretations. Louis Berent (2015) wrote an excellent white paper detailing the comparison of NSEM to Saribudak's (2012) resistivity profiles of Hockley Dome's radial fault in Katy, Texas. Lightning resistivity and permittivity data volumes are used here to generate additional interpretations of Goose Point's various datasets (Figs. 4 and 5).

The significance of verifying gas charged sediments creating zones of poor data could be indicative of active faults which leak gas and brines up the fault planes as the faults move (Kuecher et al., 2001). Lightning derived resistivity volume mapping contains some high resistivity features which may offer insight into stratigraphy (sands or limestones versus shales), potential gas accumulations, leaky zones/migration pathways along fault planes, or possibly even gas seeps. However, at this time seep data is hypothetical and not verified by resistivity measurements in the lake. This is an area for future research. The primary purpose of the sparker data in this lightning study is picking fault locations that have propagated to the surface or near surface and projecting them into resistivity and permittivity volumes to image fault planes.

Selected Attribute Discussion

Here we define in more detail the selected attributes of strike-density, rise-time, and rate-of-rise-time. Numerous historical images from Google Earth as well as from USGS Coastal Land Loss Maps (Couvillion et al., 2011) show a progression of more open water in the marshes, enlarging streams and channels in the mixed pine and oak woodland areas in between the marsh and the Lacombe Fault scarp to the north. Faulting, subsidence, sea level rise, storms and some controlled burns have likely contributed to the growth of these various water features. The LIDAR image used in this study area was shot in 1999. By changing the scales, it is possible to see many ancestral channels that were not visible in the free version provided from SONRIS. With further enhancements to the scales, limiting the elevation to between 0 and about 4 ft (1.2 m), we can see a broad spectrum of quite subtle ancestral fluvial features that are largely represented today as Bayou Lacombe and its ancestral channels and tributaries in the landscape. In the windowed area in the north central portion of the study area, we highlighted LIDAR with fine lines to assist the reader in seeing and locating landscape features for comparison in small figures. This busy image was beneficial in highlighting discrete portions of the study area and also show small features from individual lightning attributes that appear to correlate with some surface features. As shown in the following series of Figures 6–8, the common features between the attributes and the LIDAR meanders are highlighted in white. This is a first step in recognizing the apparent correlations between specific attributes and surface features. We also compare these attributes to the LGS 30 x 60 minute geologic map of the area. Features vary somewhat among the attributes. However, specific attributes better illustrate the Pleistocene boundary with the marsh or lineaments, which may correspond to a more extensive relic shoreline than previously identified.

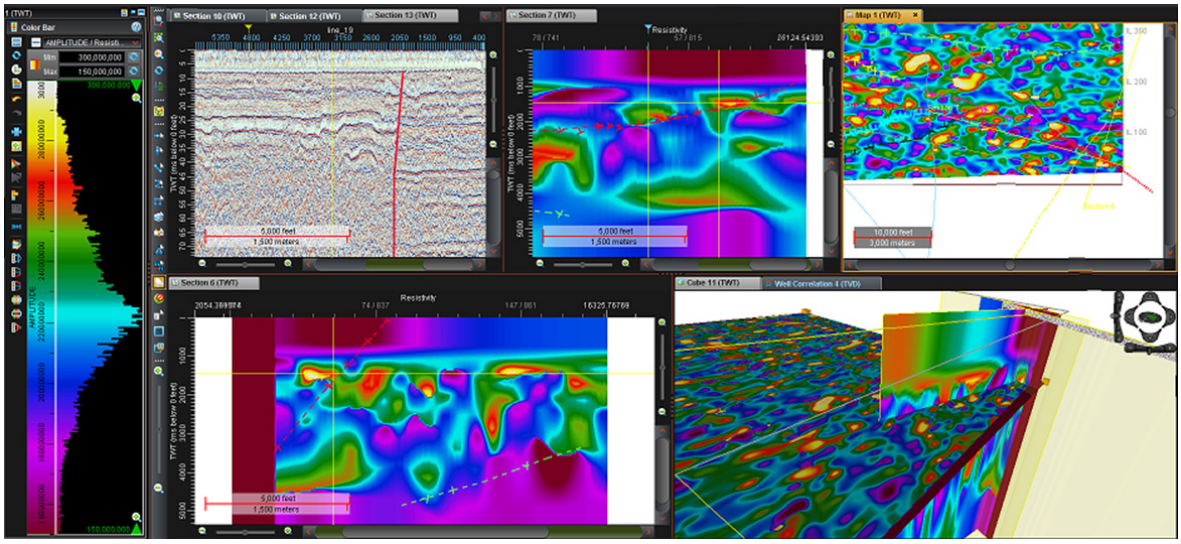

Figure 4. This is a screen shot of the integration of sparker line 19 and resistivity project analysis. Note that the sparker line sits at the top of the zone of poor data in the lower right panel.

Rise-Time

The current in a lightning strike does not rise to its maximum value instantaneously. A measurable time elapses between the first detection of energy from a lightning strike raising above the background electrical noise and that current reaches its maximum value. This time is called the rise-time, and typically ranges from 5 and 20 µs. Values of rise-time for all lightning strikes in the database are sorted into IG–7 cells and averaged. The IG–7 (Infinite Grid^{SM}) cells are 2" of longitude by 1" of latitude, or about 177 ft (54m) east-west and by 102ft (31m) north-south at 30° north latitude. This is a lot of electrical energy concentrated in a relatively small area over time. This averaging is like stacking seismic data, removing noise and improving consistent signal. The values presented in rise-time maps are in microseconds, and are typically filtered with a Gaussian filter of 1640 ft (500 m) after gridding.

Rate-of-Rise-Time

Calculating the rate of rise time is done by dividing the peak current, another unique value for each lightning strike (measured in kiloamps), by the rise-time, for each specific strike. These rate-of-rise-time values for strikes are sorted into IG–7 cells and averaged. Included maps of rate-of-rise-time show high values (those with short rise-time and large peak current) in red, while low values are violet.

Strike-Density

Strike-density is a measure of how frequently lightning strikes a specified area. It is determined by measuring the number of strikes within each IG–7 map cell over a known time interval. The area of the map cell is known, and the period of measurement is known, so an average value for a standard area for a standard time interval can be calculated. The units for this attribute are strikes per sq. km per yr. In this project, the calculation was from a database with 16.92 yr of data.

Published maps of lightning density in the Lake Pontchartrain area show an average of 10–14 lightning strikes per square kilometer per year. This density over 16 yr means there have been 160–224 lightning strikes per square kilometer per year. When we mapped the density of lightning strikes from the available databases, the maps show up to 30 lightning strikes per IG–7 grid cell per year.

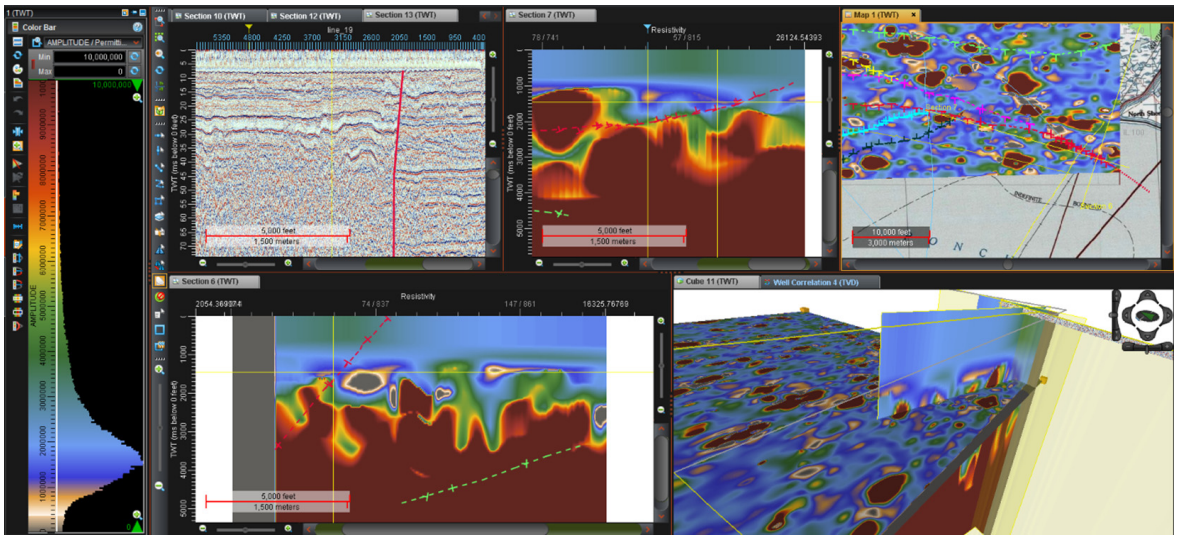

Figure 5. This is a screen shot of the integration of sparker line 19 and permittivity into the project analysis. Note that the sparker line sits at the top of the zone of poor data in the lower right panel.

Resistivity and Permittivity

The development of resistivity and permittivity volumes provides new kinds of lightning data analysis for geologic interpretations. Lightning can be modeled as the discharge of a capacitor through a resistive circuit. A capacitor is formed from two conductive plates separated by an insulating layer. The capacitor discharged by a lightning strike has one plate formed by charged water droplets in the cumulonimbus cloud and the other by the ground surface underneath the cloud. The insulating layer is the air in between.

When a lightning strike occurs, the ionized path in the air—the visible lightning stroke—is part of the electrical circuit. But though the lightning strikes the ground (usually) at a single point, the area of the capacitor can be quite large, and because the resistance of rocks is generally much higher than the resistance of ionized air, the rocks contribute the majority of the resistance encountered by the electrical current from the lightning.

When a capacitor discharges through a resistive circuit, the discharge is not instantaneous: the current decays exponentially from an initial peak, and a higher resistance means a slower discharge. We make assumptions about the dimensions of the lightning capacitor to calculate the effective resistance. This measured resistance is affected by resistivity of rocks below the surface, as well as those at the surface, and the larger the dimensions of the capacitor, the deeper the rocks involved. With reasonable assumptions about the resistivity and capacitor model, apparent resistivity values can be calculated for a location and depth which differ for each lightning strike. This forms, in effect, a sparsely sampled 3D volume of apparent resistivity values.

Interpolation of these sparsely sampled volumes can produce a regularly sampled volume suitable for display and interpretation using standard seismic interpretation software. Note that while the locations of the data used to form these volumes are quite accurate, the depths and the resistivity values depend on details of the model used in computation. So these are actually apparent resistivity and apparent depth. Given sufficient subsurface resistivity information from wells, it will be possible to calibrate both resistivity and depth.

While the decay of the capacitor discharge current depends on the resistance of the discharge circuit, a purely resistive discharge circuit would imply an instantaneous rise to peak current once the discharge path is completed. But this is not what is observed. The rise to peak current is not instantaneous, but takes place over a measurable rise time. This finite rise time implies either capacitative or inductive elements in the effective circuit. A similar effect is measured in induced polarization exploration, where it is considered to be a distributed capacitance in the subsurface given the name apparent permittivity.

Using the same model we use to compute resistivity, we can compute values for apparent permittivity as a function of location and depth, and interpolate these sparse values to give 3D apparent permittivity volumes. There may well be inductive elements in the subsurface too. But there is no way of separating them from the capacitative elements. If future lightning recording systems develop the capability to record the extended waveform of the lightning signal, more complete modeling to include capacitative, resistive, and inductive elements

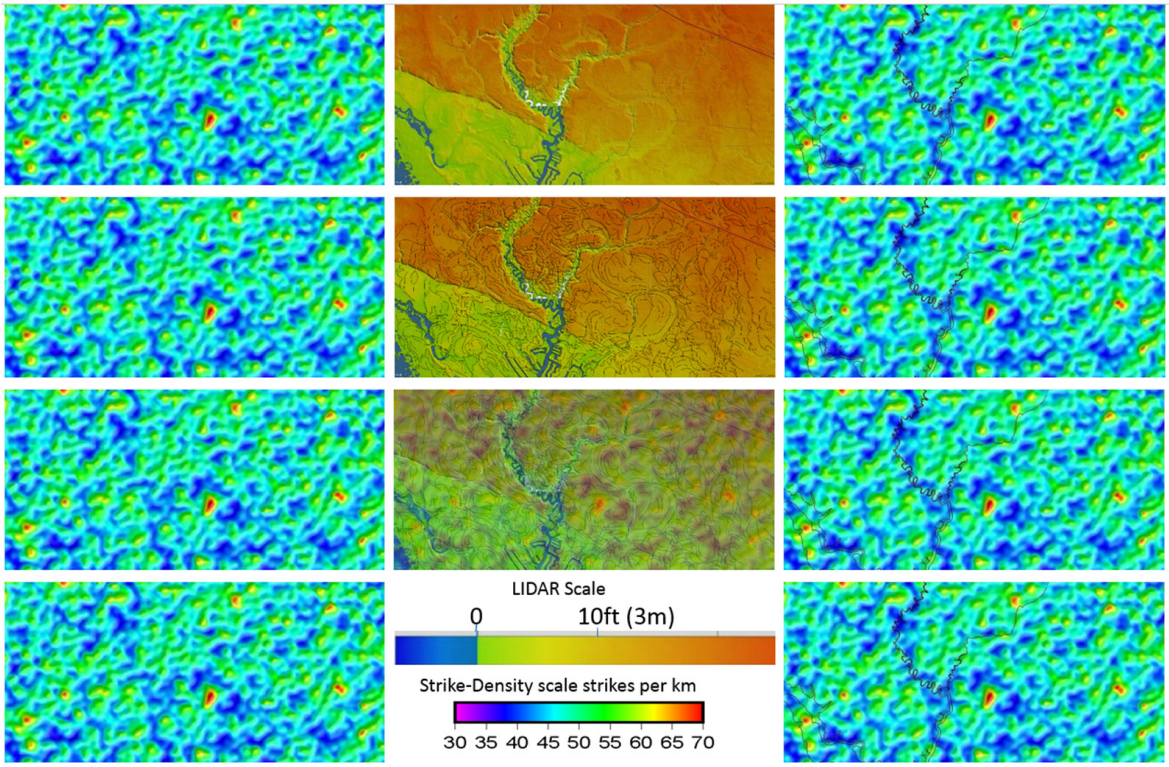

Figure 6. This panel shows the side by side comparison of strike-density and LIDAR. The column on the left shows the unannotated strike-density. The center column shows a progression of LIDAR displays. From top to bottom, finely scaled LIDAR, finely scaled LIDAR with highlighted meanders, strike-density overlay on finely scaled LIDAR with highlighted meanders, and scales. The column on the right shows the strike-density with just the channels of Bayou Lacombe and the Big Branch tributary on the top right.

should become possible (Denham, 2015; and further personal communication in 2015 with L. Denham).

The Figures 9 and 10 shown below are screen captures of resistivity and permittivity slices displayed on a Landmark DecisionSpace™ workstation. They are displayed to illustrate how this data looks and functions as a volume with in-line and cross-line views, as well as index maps and horizontal slices. These data are interpreted using the same rainbow scales as applied by surface resistivity profiling technologies imaging resistivity in the first few meters. Both of these technologies use breaks in the shallow horizons that also separate spectrum variations to interpret fault locations. The fault interpretations that rely on sparker can vary somewhat between previously mapped fault interpretations of faults in the lake. The interpretations made here projected fault picks from sparker data through the sparse near surface data zones of resistivity and permittivity to breaks in the data below. This methodology of locating shallow breaks in the rock property volumes was then extended to other areas that exhibited similar data disruption characteristics. These new interpreted fault traces derived from resistivity and permittivity offer a different and more complex view of possible fault correlations in the study area both onshore and offshore. Figure 11 shows an expanded view of the faults picked from the resistivity and permittivity volumes.

SUMMARY AND CONCLUSION

This second Goose Point study which now integrates lightning strike data is a positive step towards understanding the potential applications of lightning data when integrated with other forms of conventional geological and geophysical data. This study demonstrated the practical application of lightning derived resistivity and per-

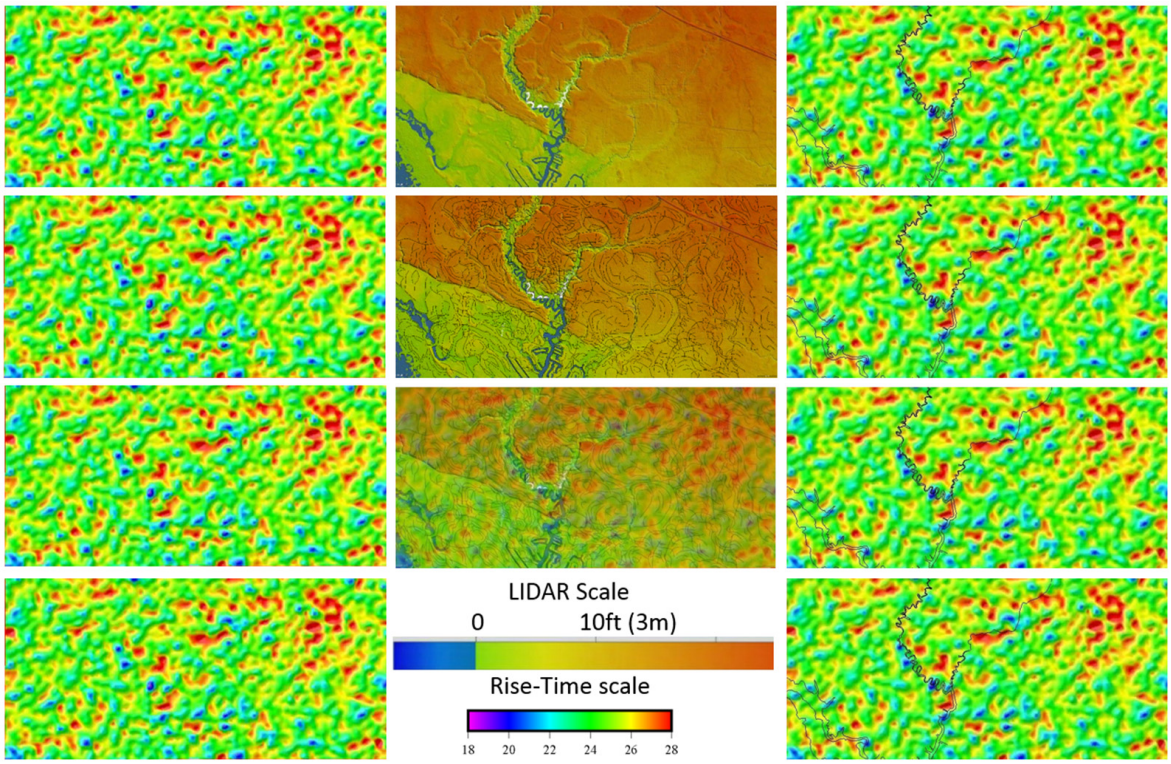

Figure 7. This panel shows the side by side comparison of rise-time and LIDAR maps. The column on the left shows the unannotated rise-time. The center column shows a progression of LIDAR displays. From top to bottom, finely scaled LIDAR, finely scaled LIDAR with highlighted meanders, and rise-time overlay on finely scaled LIDAR with highlighted meanders, and scales. The column on the right shows the rise-time with just the channels of Bayou Lacombe and the Big Branch tributary on the top right.

mittivity volumes in providing a platform to interpret sparse or fragmented conventional data types and generate reasoned interpretations. This 110 sq. mi. (285 sq. km.) study of the Goose Point area resulted in the reinterpretation of the existing mapped faults and the introduction of several possible additional faults.

Significant interpretive effort was devoted to matching the shallow sparker data derived faults to their presumed subsurface projections that were revealed in the deeper NSEM resistivity profiles. The resistivity cross-sections were extracted from 3D resistivity and permittivity volumes as arbitrary lines that traversed the same path as the sparker data. The sparker, resistivity and permittivity profiles were then displayed at the same horizontal scale and then vertically aligned to facilitate correlating similar fault patterns in the shallow and deep data. Once the shallow expression of each fault was recognized in the deeper NSEM resistivity and permittivity data, a traditional fault analyses was conducted to map the project area's fault patterns. Fault planes were also monitored and mapped in an effort to provide as much quality control of the fault analysis as possible. Faults were recognized on the NSEM data based on resistivity layer terminations and suggestions of offset.

Comparing the three lightning attribute maps of rise-time, rate-of-rise-time and strike-density with Heinrich's geologic map (Heinrich, et al., 2004) of the Goose Point project area, it appears that each attribute tends to highlight a different geologic feature.

This second Goose Point study which now integrates lightning strike data is a positive step towards understanding the potential applications of lightning data when integrated with other forms of conventional geological and geophysical data. This study demonstrated the practical application of lightning derived resistivity and permittivity volumes in providing a platform to interpret sparse or fragmented conventional data types and generate reasoned interpretations. This 110 sq. mi. (285 sq. km.) study of the Goose Point area resulted in the reinterpretation of the existing mapped faults and the introduction of several possible additional faults. Fault planes were interpreted on NSEM by projecting fault picks from sparker profiles into resistivity and permittivity volumes and

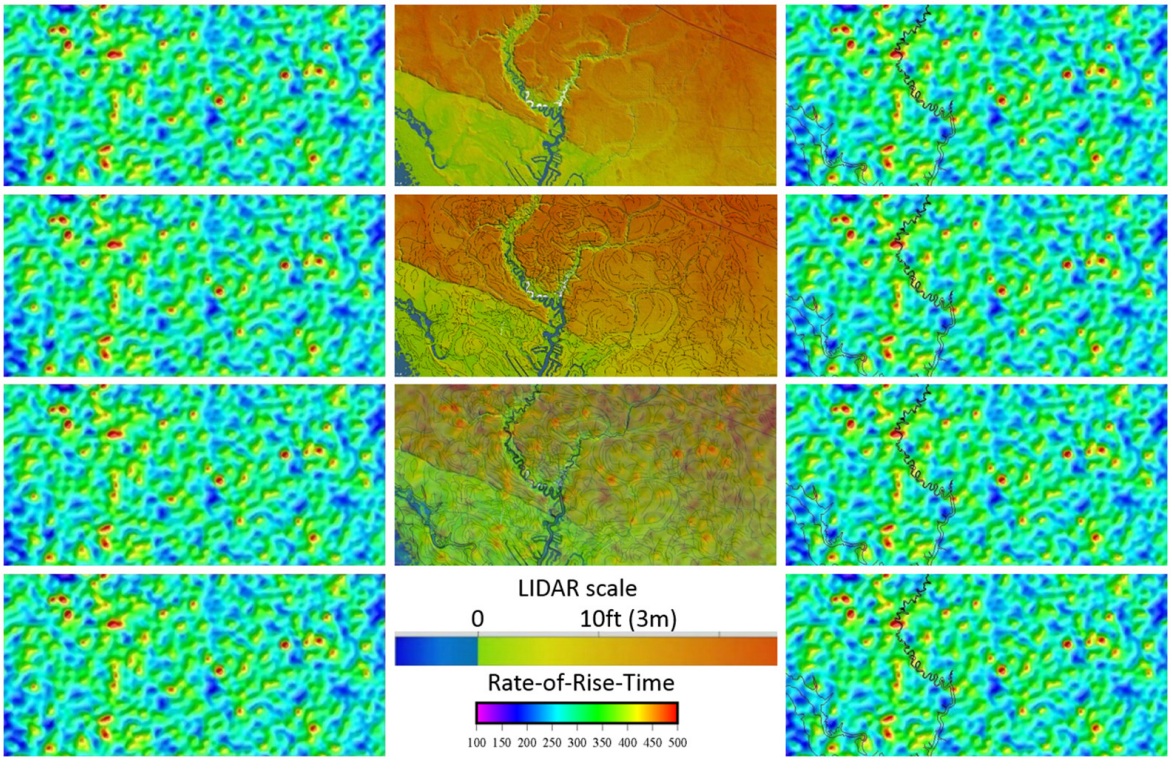

Figure 8. This panel shows the side by side comparison of rise-time and LIDAR maps. The column on the left shows the unannotated rise-time. The center column shows a progression of LIDAR displays. From top to bottom, finely scaled LIDAR, finely scaled LIDAR with highlighted meanders, rise-time overlay on finely scaled LIDAR with highlighted meanders, and scales. The column on the right shows the rise-time with just the channels of Bayou Lacombe and the Big Branch tributary on the top right.

identifying patterns in the data associated with these faults. Once the fault patterns were identified they could be recognized throughout the study area.

A comparison of a geologic map (Heinrich, et al., 2004) with three lightning attributes (rise-time, rate-of-rise-time, and strike-density), shows that the Goose Point study attributes appear to highlight some common but mostly different features. Rate-of-rise-time, (Fig. 8) best reflects the Pleistocene/Marsh interface and possibly a relic shoreline just to the south of it. This attribute also has low values in a lineament trending northwest-southeast from the tip of Goose Point to the Hwy 11 Bridge which may approximate a transform boundary described by Stephens (2010) similar to the Brazos River in Texas (Haggar, et al., 2014). Some fine straight lineament patterns in this attribute are unidentified at this time. Interestingly, three prominent dark blue/low scale value polygons on rate-of-rise-time were found to correlate to the three brightest "hot spots" on strike-density (all in wooded areas). The attraction of lightning to these locations is unknown at this time.

Strike-density (Fig. 6) like rate-of-rise-time, shows a northwest-southeast trending feature that appears to correspond to the possible transform feature that runs just offshore from Goose Point to the Hwy 11 Bridge area. Onshore we observed fine patterns that correspond to stair stepping offset features in streams that may correspond to small faults or joint patterns. (This topic needs additional research.) Broader low strike-density patterns that straddle the various shorelines and proceed into the lake seem to follow and/or parallel recent stream features suggesting stream migration.

Rise time (Fig. 7) exhibits patterns of relatively uniform intensity. There are no noticeable color gradient patterns from onshore to offshore. This attribute appears to have the best correlation to the subtle lineament associated with the Lacombe fault. Of the three attributes cited in this study, when compared to LIDAR, rise-time shows the best correlation to meander features. However, this correlation is still not developed sufficiently at this time to produce reliable maps of features.

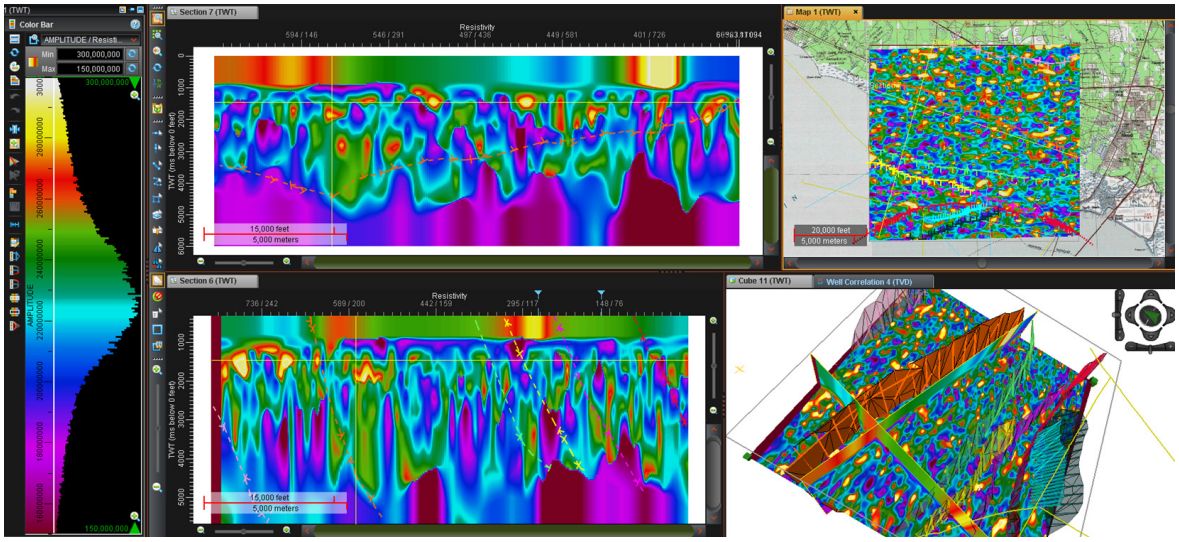

Figure 9. Screen capture of resistivity volume analysis. Resistivity colorbar is on the left. Top center shows resistivity volume strike line just south of the Lacombe Fault, orange fault. Bottom center shows resistivity volume dip line across the Lacombe Fault, orange fault. This dip line also shows additional interpreted faults based on the pattern of resistivity disturbance shown in the orange fault on this line. The upper right quad map shows a horizontal slice of resistivity at 1456 ms (approx. 5100 ft or 1554 m) over the study area with fault traces projected to this surface. Note the resistivity volume fault interpretation resulted in several possible new faults mapped in addition to the ones only mapped with sparker. Perhaps some of these faults do not reach the surface or as shallow as the sparker. The vertical calibration of resistivity and Permittivity volumes is still being evaluated. The lower left image is a rotated view 45 degrees counter clockwise compared to the image in the upper right. In this cube image, the horizontal resistivity slice is at 1456 ms with fault planes highlighted. The red fault on the right is the fault that cuts the Hwy. 11 Bridge. It appears to develop a horse tail pattern of additional faults to the northwest shown in purple and yellow as well as 2 compensators to the southeast shown in aqua and gray. The green fault and the pink fault do not intersect any other mapped faults. This resistivity based fault interpretation offers a different alignment of the Goose Point Fault (s) between Goose Point and the Hwy. 11 Bridge.

Rate-of-rise-time (Fig. 8) best reflects the Pleistocene/Marsh interface and possibly a remnant of a relic shoreline just to the south. This attribute also has low values in a lineament trending northwest-southeast from the tip of Goose Point to the Hwy 11 Bridge which may approximate a transform boundary described by Stephens (2010) similar to the Brazos River in Texas (Haggar, et al., 2014). This attribute exhibits several straight lineament patterns that have not yet been correlated to geology. The three prominent dark blue (low rise time rate) polygons were found to correlate to wooded areas as well as to the three brightest "hot spots" on the strike-density attribute map. Lightning's attraction to these wooded areas still may still turn out to be related to local geology, which in turn would have influenced soil formation and subsequent tree growth. These correlations are currently being investigated.

Overall, these Goose Point attributes did not appear to provide definitive trends or mappable features like those observed in a similar NSEM study in Texas. That study imaged a stream system in some detail, or roughly aligned with the Brazos River, or imaged some surface fault segments northeast the Brazos River area. (Haggar et al., 2014). The Goose Point data suggests that the local surface and near surface geology controls the locations and the quality of interpretable results from NSEM attributes.

Previous studies using sparker data augmented by cores have concluded that the northeastern end of Lake Pontchartrain has active faults, including the Goose Point Fault (Kindinger et al, 1998, Roth, 1999, and Lopez, 1996-97). The reprocessed high resolution sparker lines assisted in improving the data in poor data zones to better interpret surface faults. (Fig. 3) However, some areas could not be improved possibly due to gas and/or highly disturbed bottom sediments that had been dredged for shells or sand (Kindinger et al., 1998, and Roth, 1999). Fault picks were derived from the USGS' original published sparker lines which was reprocessed. These picks

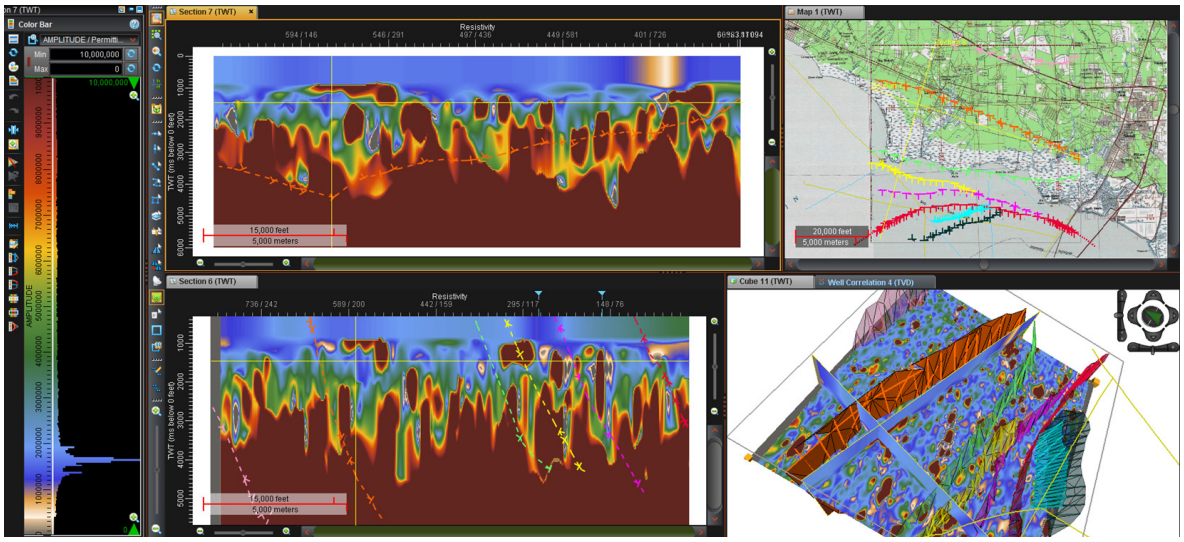

Figure 10. This is a screen capture of a permittivity volume at the same line and cross line location as the resistivity image above. Left is a color bar similar to Instantaneous Potential surveys. Top center shows a permittivity volume strike line just south of the Lacombe Fault, orange fault. Bottom center shows a permittivity volume dip line across the Lacombe Fault, orange fault. This dip line also shows additional interpreted faults based on the patterns in the permittivity. The upper right quad overlay map shows just the outline of the study area with fault traces projected to this surface. Lower right image is the same horizontal slice and faults as above, however these are now rotated and projected through the permittivity volume.

furnished surface location controls to interpret faults from resistivity and permittivity data in the sub-surface. Horizontal scales for resistivity and permittivity volumes are well established, however, we are in the process of further calibrating our 3D volumes to depth. We are also in the process of calibrating our apparent relative resistivity values to well log data and similarly looking to calibrate our relative permittivity values to induced polarization data.

Interpretation of resistivity and permittivity data is generally similar to that of near-surface conventional resistivity and induced polarization surveys where lateral discontinuities and offsets are often used to identify faults and lithologic boundaries. A recent proof of concept study performed by Louis Berent, currently being prepared for publication, compares NSEM resistivity profiles to conventional 2-D resistivity imaging across several well-known active growth faults in the Hockley-Tomball area.

Additional faults were interpreted from the lightning resistivity volumes based on similar breaks and color pattern changes in the resistivity and permittivity data across the entire study area.

Our investigation of the Goose Point study area resulted in reinterpreted fault patterns and the possible identification of additional faults where the sparker data quality was poor to questionable. While lightning data would not be expected to have better resolution than sparker data, it can identify known faults and provide a rational basis for proposing possible faults.

Strike-density, rate-of-rise-time, and rise-time attributes collectively provide insight into the location of recent and ancestral channels and channel features, relic beaches and shorelines. These lightning attributes here at Goose Point can also differentiate marsh from more consolidated sediments, show weak lineaments for some faults and slightly stronger correlations for lineaments associated with possible transforms.

Since lightning is continuously recorded, these data sets will continue to grow over time. Improvements in NSEM data quality will continue, both from enhancements in lightning acquisition techniques, and from advances in NSEM data processing. Ongoing client projects, collaboration with the state geological surveys, and university studies will provide the opportunity to further integrate NSEM with well log, seismic, subsurface, potential field data, and other surface geophysical techniques.

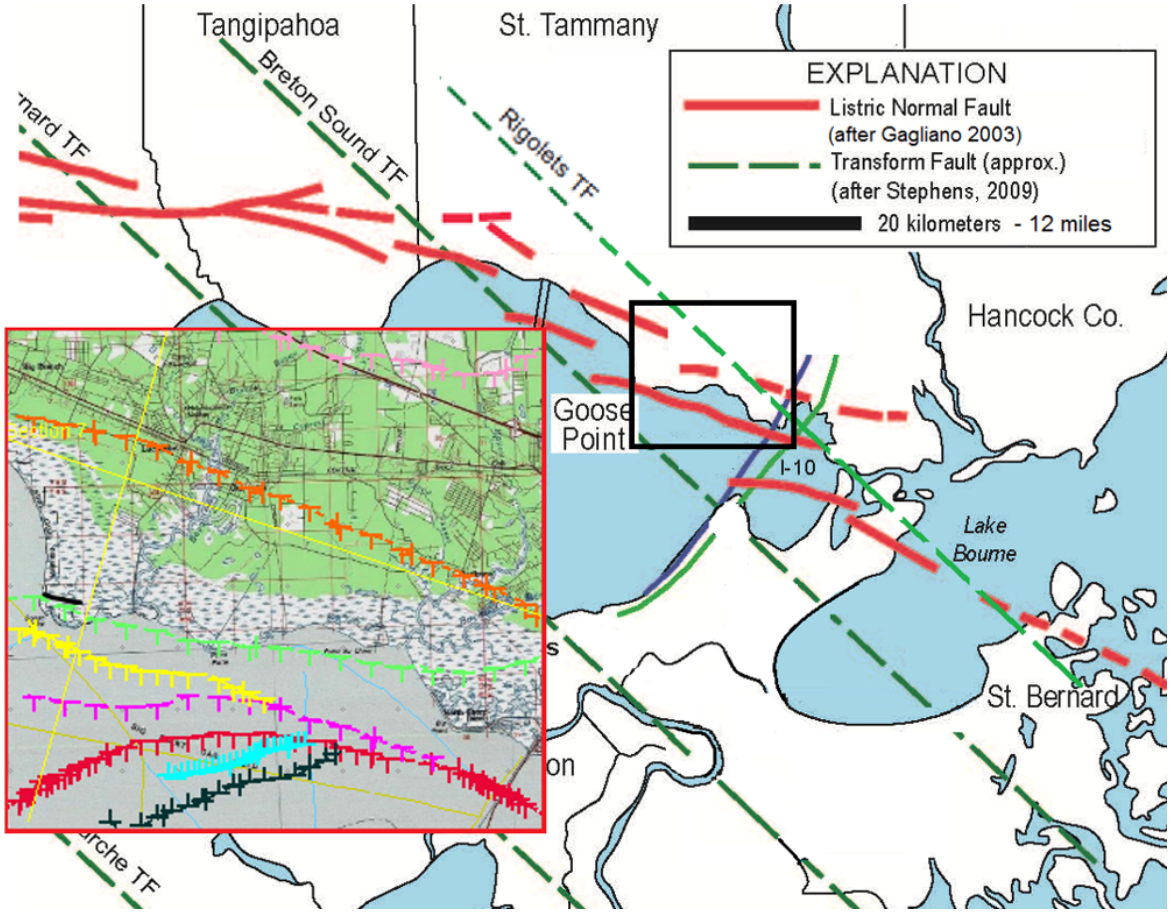

Figure 11. This side by side comparison of the published mapped faults in the study area with faults interpreted from resistivity and permittivity volumes generated from NSEM/lightning data. The mapped faults are picked from sparker, cores and surface breaks and offsets. Fault interpretations from lightning derived resistivity and permittivity do not violate any of the existing data, such as; previously picked faults from the surface expressions of the faults/cores, or sparker lines with the exception of the slightly different location of the fault pick in the reprocessed line 19. Roth's (1999) pick is very slightly to the north of the fault picked from our reprocessed sparker data. All of the faults mapped are down to the south except the aqua and gray faults which are down to the north compensators to the red fault. This interpretation also extends the Lacombe Fault to the east in the subsurface.

ACKNOWLEDGMENTS

Lightning data requires creative adaptive applications of work station technology. H. Roice Nelson, Jr., a founder of Landmark Graphics, used the new Landmark DecisionSpace™ to generate numerous screen captures and illustrations essential to the interpretation of resistivity and permittivity volume data and for the figures in this paper. Mr. Kelly Haggar is also recognized for providing assistance with location information and figures.

REFERENCES CITED

Aminzadeh, F., P. de Groot, T. Berge, and G. Valenti, 2001, Using gas chimneys as an exploration tool: World Oil magazine, May 2001 issue, p. 50–56.

Berent, L. J., 2015, Mapping faults with lightning, natural-sourced electromagnetics (NSEM)—Validating NSEM with 2-D resistivity imaging profiling and ground penetrating radar: Dynamic Measurement, LLC White Paper, Barker, Texas, <http://www.dynamicmeasurement.com/TAMU> Accessed June 27, 2015.

Couvillion, B. R., J. A Barras, G. D. Steyer, W. Sleavin, M. Fischer, H. Beck, N. Trahan, B. Griffin, and D. Heckman, 2011, Land area change in coastal Louisiana from 1932 to 2010: U.S. Geological Survey Scientific Investigations Map 3164, scale 1:265,000, 12 p. pamphlet.

Denham, L., 2015, Using lightning for exploration: Geophysical Society of Houston, Texas, presentation to the potential fields special interest group on January 15, 2015.

Gagliano, S., B. Kemp, K. Wicker, and K. Wiltenmuth, 2003, Active geological faults and land change in southeastern Louisiana: A study of the contribution of faulting and land change in southeastern Louisiana: A study of the contribution of faulting to relative subsidence rates, land loss, and resulting restoration projects, <http://www.coastalenv.com/Active_Geological_Faults_and_Land_Change_in_SE_LA.pdf > Accessed March 23, 2015.

Haggar, K. S., R. Nelson, J. Seibert, and L. Denham, 2014, Aquifers, faults, and subsidence and the lightning database. Gulf Coast Association of Geological Societies Transactions, v. 64, p. 139-159.

Heinrich, P. V., R. P. McCulloh, and J. Snead, 2004, Gulfport 30x60 minute geological quadrangle: Louisiana Geological Survey, Baton Rouge, <http://www.lgs.lsu.edu/deploy/uploads/Gulfport%20100K.pdf> Accessed March 10, 2015

Kindinger, J. L., 1998, Holocene geologic framework of Lake Pontchartrain Basin and lakes of southeastern Louisiana, <http://pubs.usgs.gov/of/1998/of98-805/html/kindingr.htm> Accessed March 23, 2015.

Kuecher, G. J., H. H. Roberts, M. D. Thompson, and I. Mathews, 2001, Evidence for active growth faulting in the Terrebonne delta plain, south Louisiana: Implications for wetland loss and the vertical migration of petroleum: Environmental Geosciences, v. 8, p. 77–94.

Kulp, M., P. Howell, and J. Lopez, 2002, Baton Rouge–Denham Springs Fault System, Lake Pontchartrain, *in* S. Penland, A. Bell, and J. Kindinger, eds., 2002 environmental atlas of the Lake Pontchartrain Basin: U.S. Geological Survey, Open-File Report 02–206, <http://pubs.usgs.gov/of/2002/of02-206/geology/fault-system.html> Accessed 23 March, 2015

Lee, M. W., 2004, Elastic velocities of partially gas-saturated unconsolidated sediments. Marine and Petroleum Geology v. 21, p. 641–650.

Lopez, J. A., 1996, Review and update of active geologic faulting in Lake Pontchartrain: 3rd Bi-Annual Basics of the Basin Research Symposium, New Orleans, Louisiana <http://www. saveourlake.org/PDF-documents/BOB/BasicsofhteBasinProceedings1996.pdf> Accessed March 3, 2015.

Lopez, J. A., S. Penland and J. Williams, 1997, Confirmation of active geologic faults in Lake Pontchartrain in southeast Louisiana: Gulf Coast Association of Geological Societies Transactions, v. 47, p. 299–303.

Nelson, H. R., Jr., L. Denham, and J. Seibert, 2014, Lightning data, a new geophysical data type: American Association of Petroleum Geologists Search and Discovery Article 41184, Tulsa, Oklahoma, <http://www.searchanddiscovery.com/pdfz/documents/2013/41184nelson/ndx_nelson.pdf.html> Last accessed September 6, 2015.

Saribudak, M., 2011, Geophysical mapping of the Hockley growth fault in northwest Houston, USA, and recent surface observations: The Leading Edge, v. 30, p. 936–943.

Seibert, J., 2015, Lightning discoveries and technologies: Electricity Today, January-February 2015 issue.

Stephens, B. P., 2009, Basement controls on subsurface geologic patterns and coastal geomorphology across the northern Gulf of Mexico: Implications for subsidence studies and coastal restoration: Gulf Coast Association of Geological Societies Transactions, v. 59, p. 729–751.

Stoessell, R. K., and L. Prochaska, 2005, Chemical evidence for migration of deep formation fluids into shallow aquifers in south Louisiana: Gulf Coast Association of Geological Societies Transactions, v. 55, p. 794–808.